Published in final edited form as:
Nano Lett. 2012 July 11; 12(7): 3587–3591. doi:10.1021/nl301253v.

Mass production and size control of lipid-polymer hybrid nanoparticles through controlled microvortices

YongTae Kim[1], **Bomy Lee Chung**[1,2], **Mingming Ma**[1], **Willem J. M. Mulder**[4], **Zahi A. Fayad**[4], **Omid C. Farokhzad**[5], and **Robert Langer**[1,2,3,*]

YongTae Kim: ytkim@mit.edu; Bomy Lee Chung: bomy@mit.edu; Mingming Ma: mmma@mit.edu; Willem J. M. Mulder: willem.mulder@mountsinai.org; Zahi A. Fayad: zahi.fayad@mssm.edu; Omid C. Farokhzad: ofarokhzad@zeus.bwh.harvard.edu

[1]David H. Koch Institute for Integrative Cancer Research, Massachusetts Institute of Technology, Cambridge, Massachusetts 02139, USA

[2]Department of Chemical Engineering, Massachusetts Institute of Technology, Cambridge, Massachusetts 02139, USA

[3]Harvard-MIT Division of Health Sciences and Technology, Massachusetts Institute of Technology, Cambridge, Massachusetts 02139, USA

[4]Translational and Molecular Imaging Institute, Mount Sinai School of Medicine, One Gustave L. Levy Place, Box 1234, New York, 10029, USA

[5]Department of Anesthesiology, Brigham and Women's Hospital, Harvard Medical School, Boston, Massachusetts 02115, USA

Abstract

Lipid-polymer hybrid (LPH) nanoparticles can deliver a wide range of therapeutic compounds in a controlled manner. LPH nanoparticle syntheses using microfluidics improve the mixing process, but are restricted by a low throughput. In this study we present a pattern-tunable microvortex platform that allows mass production and size control of LPH nanoparticles with superior reproducibility and homogeneity. We demonstrate that by varying flow rates (i.e. Reynolds number (30~150)) we can control the nanoparticle size (30~170nm) with high productivity (~3g/hour) and low polydispersity (~0.1). Our approach may contribute to efficient development and optimization of a wide range of multicomponent nanoparticles for medical imaging and drug delivery.

Keywords

nanoparticle; microvortex; synthesis; control; polymer; microfluidics

Institute Professor Robert Langer, David H. Koch Institute for Integrative Cancer Research, Massachusetts Institute of Technology, 77 Massachusetts Avenue, Room 76-661, Cambridge, Massachusetts 02139-4307, (phone) 617-253-3107, (fax) 617-258-8827, rlanger@mit.edu.

Supporting Information **Available.** Supporting information with 5 figures and a table includes microfluidic device design and fabrication, flow control and Reynolds number calculation, flow visualization and microscopy, numerical simulations, material preparation of nanoparticle synthesis, particle sizing, and transmission electron microscopy (TEM). This material is available free of charge via the Internet at http://pubs.acs.org.

Conflict of Interest Disclosure: In compliance with the Brigham and Women's Hospital and Harvard Medical School institutional guidelines, O.C.F. discloses his financial interest in BIND Biosciences and Selecta Biosciences, two biotechnology companies developing nanoparticle technologies for medical applications. BIND and Selecta did not support the aforementioned research, and currently these companies have no rights to any technology or intellectual property developed as part of this research.

Biodegradable, drug-encapsulated polymeric nanoparticles can be synthesized using established methods such as nanoprecipitation[1, 2]. Nanoprecipitation techniques vary nanoparticle design parameters to adjust the physicochemical features such as drug loading and nanoparticle stability, as well as biological features such as cellular specificity[3-6]. However, conventional bulk techniques, which involve dropwise addition of polymers in an organic solution to a water-based solution, have faced critical challenges that include poor reproducibility, polydisperse size distribution, and batch-to-batch variations in nanoparticle physicochemical properties[7-9]. These problems mainly result from the inability to control the mixing processes required for nanoparticle syntheses because bulk methods involve macroscopic mixing of precursor solutions although their microscale interactions determine nanoparticle formation and characteristics[10, 11]. Highly controlled microscale mixing processes that can produce targeted nanoparticles with optimal physicochemical properties are needed.

Continuously focused laminar flows in microfluidics (e.g. two-dimensional (2D) hydrodynamic focusing[12]) have been used to synthesize a diversity of micro/nanoparticles[13-17]. In these approaches, lateral diffusive dispersion across the interface of parallel streams flowing alongside in microfluidics induces relatively controlled mixing of nanoparticle precursors compared to conventional bulk methods. For example, an approach to controlled synthesis of PLGA-PEG polymeric nanoparticles, which has the ability to regulate single-step nanoprecipitation, was developed for nanoparticle-facilitated drug delivery[10]. This approach has been advanced using three-dimensional (3D) focusing flow patterns to prevent localized PLGA aggregation near the polydimethylsiloxane (PDMS) microfluidic channel walls[18]. While these approaches have provided significant advantages, there still remain challenges. First, these microfluidic approaches using slow diffusive mixing at a low flow rate (i.e. a low Reynolds number, a ratio of inertial to viscous forces; see Supporting Information) are basically limited to low productivity without complicated fabrication for high-throughput platforms. Second, diffusive mixing does not allow the development of particles that require the assembly of precursors (e.g. lipid) in the aqueous phase with precursors (e.g. polymer) in the organic phase such as lipid-polymer hybrid nanoparticles. Third, large-scale nanoparticle production using slow passive mixing requires long storage of the produced nanoparticles with organic solvent (e.g. acetonitrile), which may cause unnecessary polymer aggregation or undesired variations in physicochemical properties[4, 5, 19].

To overcome these challenges and obtain a high-throughput and reproducible nanoparticle synthesis technology, rapid mixing of nanoparticle precursors is required and the mixing process needs to be highly controlled. A diverse range of inertial microfluidic platforms have been designed for rapid convective mixing, 3D focusing patterns, and dynamic particle manipulation[20-30]. Recently, it has been demonstrated that rapid mixing in a Tesla-type microfluidic structure results in improved formation of lipid-polymeric nanoparticles[19]. However, high-throughput nanoparticle synthesis with high reproducibility still remains a challenge. In the current study, we develop a controllable microvortex platform for the synthesis of LPH nanoparticles with high productivity and reproducibility. We predict and manipulate 3D fluid flow patterns in the microfluidic channel to regulate tunable microvortex formation for rapid mixing and controlled nanoprecipitation. We demonstrate that, by varying microvortex patterns with defined polymer-lipid compositions and concentrations, we can control and optimize the nanoparticle size.

LPH nanoparticles were synthesized by rapidly mixing an organic solution of PLGA (polymer) dissolved in acetonitrile in the central inlet and a 4% ethanol aqueous solution containing lecithin (lipid) and DSPE-PEG (lipid-PEG) in the outer inlets in a single layer, 3-inlet microfluidic channel, which generated microvortices at a relatively higher Reynolds

number regime (Re~75) than used in conventional microfluidics (Re~1) (Figure 1a, 1b and S1; for detailed device specification and Reynolds number calculation see Supporting Information). The nanoparticles synthesized in the microvortices have a polymeric core of PLGA and a lipid corona of lecithin and DSPE-PEG (Figure 1c)[4, 5]. These hybrid nanoparticles combine the unique strengths of liposomal and polymeric nanoparticles while overcoming their limitations in terms of drug encapsulation efficiency and storage stability. Compared to pure PLGA-PEG nanoparticles[10, 18], these lipid-polymer hybrid nanoparticles exhibit a higher drug loading and slower drug release[3-6].

Symmetric microvortices are created at the intersection of the three inlets (Figure 1a and S2), where the upstream profiles show the inner shapes of two symmetric microvortices, which results in rapid mixing of polymer and lipid (Figure 1b; see plane 1 and 2), while the downstream patterns exhibit 3D diamond-like focusing patterns that can prevent polymer aggregation near the channel walls, preventing the channel from clogging (Figure 1b; see plane 3 and 4). The use of microvortices enabled up to 1000 times higher productivity than previous approaches using diffusive mixing[10] and convective mixing[19] (Figure 1d). Nanoparticle productivity achieved in this microfluidic device was given as a function of the flow rate (i.e. the Reynolds number) and the PLGA concentration (Table 1 and Figure S3; for detailed experimental conditions see Supporting Information). The size of LPH nanoparticles was controlled by varying the Reynolds number (Figure 1e, 1f, and 1g), while maintaining the other parameters constant. Nanoparticle imaging and size measurement were performed after a previously reported purification process[4, 5] (see Supporting Information).

We investigated the nanoparticle size by varying the Reynolds number (30, 75, and 150) while maintaining constant PLGA-to-lipid weight ratios of 5, 10, 25, 50, and 100 (Figure 2a). We simulated and predicted desired flow patterns using computational fluid dynamics (CFD) and visualized them with a stereo-microscope (for details see Supporting Information), which demonstrated various flow patterns including controlled microvortices at Re=3, 30, 75, and 150 with three different flow rate ratios of 1:5, 1:10, and 1:20 (Figure S5). We observed that an increase in the Reynolds number results in a decrease in the nanoparticle size at the given PLGA-to-lipid ratio. For example, the variation of the Reynolds number from 30 to 150 with a PLGA-to-lipid ratio of 10 resulted in a size decrease from 93 to 55 nm (Figure 2a; see Table S1). This illustrated that by varying flow rates in our microvortex platform the nanoparticle size could be reliably controlled, while keeping the same polymer-lipid composition. We also observed that this size control is less predictable and controllable at both high and low PLGA-to-lipid ratios (Figure 2a). A minimal size of 20 nm was achieved at a ratio of 5 with high Reynolds numbers (Re=75 or 150). Increasing the PLGA-to-lipid ratio to 100 resulted in an increased nanoparticle size at a Reynolds number of 30, where the microvortex patterns are not strong enough to mix the excessive polymer with lipid efficiently. This size map indicated that varying these two parameters could produce the nanoparticles in a size range of 30 to 170 nm. This size range of the nanoparticle can be extended by varying the design parameters of the device or the polymer-lipid compositions. In this study, we have targeted the nanoparticle size between 50 and 150 nm, which may be an ideal range for stable and biologically relevant nanoparticles[3, 6].

Simulation of the flow patterns demonstrated that convective mixing between polymer and lipid is not dominant enough for nanoparticle synthesis at lower Reynolds number (Re=3) due to underdeveloped microvortex patterns, whereas the higher Reynolds numbers (Re>30) provide strong and rapid convective mixing (Figure S5). We compared the variation of the nanoparticle size with the patterns of the microvortices (Figure 2b and 2c). Underdeveloped microvortex did not completely mix the polymer and lipid at Re=30, which can cause

aggregation at higher polymer concentrations, resulting in wide nanoparticle size distributions. In contrast, rapid convective mixing by microvortices (Re=75 or 150) resulted in narrow size distributions. Moreover, it was observed that the size changes were more sensitive to the Reynolds number than the polymer-lipid compositions, indicative of the importance of the mixing speed (i.e. Reynolds number). The abrupt decrease in the size at the PLGA-to-lipid ratio of 5 can be explained by precluded polymer aggregation as a result of excessive lipid, as previously reported[4, 5]. This result illustrates that LPH nanoparticles rapidly synthesized in the microvortex platform not only have similar characteristics to those assembled in bulk approaches, but also exhibit similar physicochemical properties, which can be readily controlled with simple flow rate changes, without the need for adjusting polymer-lipid compositions.

To gain more insight into the role of microvortex patterns in nanoparticle formation we varied the flow rate ratios of [PLGA stream] to [outer lipid streams] while varying the Reynolds number as well (Figure 3). Changing flow rate ratios from 1:10 to 1:20 did not appear to have a notable effect on the nanoparticle size at PLGA-to-lipid ratios of 10, 25, and 50 (Figure 3a), indicating that nanoparticle assembly relied on well-developed microvortices. As demonstrated above (Figure 2), an increase in the PLGA-to-lipid ratio at a constant flow rate ratio led to an increase of nanoparticle size (Figure 3b) at all the flow rate ratios, but this increase was higher at the flow rate ratio of 1:5 (Figure 3b) where microvortex patterns were not well developed due to relatively higher portion of the central stream in this microfluidic dimension (Figure 3c). This high sensitivity of the size to the PLGA-to-lipid ratio was also noted at the low Reynolds number (Re=30) (Figure 3a and 3b) where the inertial forces were not strong enough to fully develop the microvortex patterns (Figure 3c). This resulted in larger nanoparticles, which can be explained, in part, by polymer aggregation and poor mixing (Figure 3c). We found that the optimal range of the flow rate ratios in this device is between 1:10 and 1:20 for high performance of nanoparticle syntheses.

To examine the performance of nanoparticle syntheses by a conventional bulk method[4, 5] and our microvortex approach, we compared the nanoparticle size (Figure 4a), polydispersity (Figure 4b), and average size distribution (Figure 4c and 4d) using PLGA-to-lipid ratios of 10, 25, and 50. These approaches demonstrated a similar increase in nanoparticle size when the PLGA-to-lipid ratio was increased (Figure 4a). However, the synthesis by the conventional bulk method produced larger nanoparticles (80 to 120 nm; see Figure 4a and 4c) than those by our microvortex approach (Re=150) (55 to 80 nm; see Figure 4a and 4d). The bulk synthesis method resulted in nanoparticle batches that were characterized by a much wider size distribution that had multiple peaks and higher polydispersity (~0.2) (Figure 4b and 4c). In contrast, our approach using microvortex-induced rapid mixing resulted in a relatively narrow size distribution that had lower polydispersity (~0.1) (Figure 4b and 4d). This monodisperse nanoparticle fraction produced by the microvortex platform represented more than 85% of their overall volume for all PLGA-to-lipid ratios, except at 5 (Figure S4). We note that the free lipids were removed by the purification process and did not significantly affect the size (distribution) of the main LPH nanoparticle formation because rapid convective mixing in the self-assembly of LPH nanoparticles induces uniform lipid and lipid-PEG coverage around polymeric cores[19].

In this study, we demonstrated that LPH nanoparticles can be produced up to 1000 times faster than conventional microfluidic diffusive syntheses. The particle size can be readily controlled with simple changes of flow rates in our microvortex platform. We predicted a desired range of Reynolds numbers (30~150) that can generate and control the patterns of microvortices, and identified an optimal input ratio of the precursors. As compared to conventional approaches, our methodology resulted in an improved reproducibility and

homogeneity (polydispersity of ~0.1) of the nanoparticle batches. High productivity (3g/hour) and size control (30~170nm) are prerequisite for drug nanoparticle formulations to be employed for *in-vivo* applications. Our approach can facilitate good manufacturing practice (GMP) production and clinical translation.

Supplementary Material

Refer to Web version on PubMed Central for supplementary material.

Acknowledgments

This research was supported by the National Heart, Lung, and Blood Institute, National Institutes of Health, as a Program of Excellence in Nanotechnology (PEN) Award, Contract #HHSN268201000045C, National Cancer Institute Grant CA151884, and the David H. Koch–Prostate Cancer Foundation Award in Nanotherapeutics. We thank MIT Microsystems Technology Laboratory (MTL) for the use of the fabrication equipment and MIT Center for Materials Science and Engineering (CMSE) for the use of Transmission Electron Microscopy. We also thank Dr. Rohit Karnik, Dr. Robert Steward, Dr. Jong-Min Lee, Pedro Valencia, and Hyunjung Kim for scientific discussion and insightful comments.

References

1. Schubert S, Delaney JT, Schubert US. Soft Matter. 2011; 7(5):1581–1588.
2. Chan JM, Valencia PM, Zhang L, Langer R, Farokhzad OC. Methods in molecular biology (Clifton, NJ). 2010; 624:163–75.
3. Shi JJ, Xiao ZY, Kamaly N, Farokhzad OC. Accounts of Chemical Research. 2011; 44(10):1123–1134. [PubMed: 21692448]
4. Zhang L, Chan JM, Gu FX, Rhee JW, Wang AZ, Radovic-Moreno AF, Alexis F, Langer R, Farokhzad OC. Acs Nano. 2008; 2(8):1696–1702. [PubMed: 19206374]
5. Chan JM, Zhang L, Yuet KP, Liao G, Rhee JW, Langer R, Farokhzad OC. Biomaterials. 2009; 30(8):1627–34. [PubMed: 19111339]
6. Kamaly N, Xiao Z, Valencia PM, Radovic-Moreno AF, Farokhzad OC. Chem Soc Rev. 2012; 41(7):2971–3010. [PubMed: 22388185]
7. Jahn A, Vreeland WN, DeVoe DL, Locascio LE, Gaitan M. Langmuir. 2007; 23(11):6289–6293. [PubMed: 17451256]
8. Xu Q, Hashimoto M, Dang TT, Hoare T, Kohane DS, Whitesides GM, Langer R, Anderson DG. Small. 2009; 5(13):1575–81. [PubMed: 19296563]
9. Rondeau E, Cooper-White JJ. Langmuir. 2008; 24(13):6937–45. [PubMed: 18510374]
10. Karnik R, Gu F, Basto P, Cannizzaro C, Dean L, Kyei-Manu W, Langer R, Farokhzad OC. Nano Lett. 2008; 8(9):2906–12. [PubMed: 18656990]
11. Hong JS, Stavis SM, DePaoli Lacerda SH, Locascio LE, Raghavan SR, Gaitan M. Langmuir. 2010; 26(13):11581–8. [PubMed: 20429539]
12. Wu ZG, Nguyen NT. Sensors and Actuators B-Chemical. 2005; 107(2):965–974.
13. Kolishetti N, Dhar S, Valencia PM, Lin LQ, Karnik R, Lippard SJ, Langer R, Farokhzad OC. Proc Natl Acad Sci U S A. 2010; 107(42):17939–44. [PubMed: 20921363]
14. Chang Z, Serra CA, Bouquey M, Kraus I, Li S, Kohler JM. Nanotechnology. 2009; 21(1):015605. [PubMed: 19946165]
15. Jahn A, Stavis SM, Hong JS, Vreeland WN, DeVoe DL, Gaitan M. ACS Nano. 2010; 4(4):2077–87. [PubMed: 20356060]
16. Martin-Banderas L, Flores-Mosquera M, Riesco-Chueca P, Rodriguez-Gil A, Cebolla A, Chavez S, Ganan-Calvo AM. Small. 2005; 1(7):688–92. [PubMed: 17193506]
17. Sounart TL, Safier PA, Voigt JA, Hoyt J, Tallant DR, Matzke CM, Michalske TA. Lab Chip. 2007; 7(7):908–15. [PubMed: 17594011]
18. Rhee M, Valencia PM, Rodriguez MI, Langer R, Farokhzad OC, Karnik R. Advanced Materials. 2011; 23(12):H79–H83. [PubMed: 21433105]

19. Valencia PM, Basto PA, Zhang L, Rhee M, Langer R, Farokhzad OC, Karnik R. ACS Nano. 2010; 4(3):1671–9. [PubMed: 20166699]
20. deMello AJ. Nature. 2006; 442(7101):394–402. [PubMed: 16871207]
21. Lee MG, Choi S, Park JK. Lab on a Chip. 2009; 9(21):3155–3160. [PubMed: 19823733]
22. Mao XL, Lin SCS, Dong C, Huang TJ. Lab on a Chip. 2009; 9(11):1583–1589. [PubMed: 19458866]
23. Chang CC, Huang ZX, Yang RJ. Journal of Micromechanics and Microengineering. 2007; 17(8): 1479–1486.
24. Nguyen NT, Wu ZG. Journal of Micromechanics and Microengineering. 2005; 15(2):R1–R16.
25. Liu SJ, Wei HH, Hwang SH, Chang HC. Phys Rev E Stat Nonlin Soft Matter Phys. 2010; 82(2 Pt 2):026308. [PubMed: 20866906]
26. Stott SL, Hsu CH, Tsukrov DI, Yu M, Miyamoto DT, Waltman BA, Rothenberg SM, Shah AM, Smas ME, Korir GK, Floyd FP Jr, Gilman AJ, Lord JB, Winokur D, Springer S, Irimia D, Nagrath S, Sequist LV, Lee RJ, Isselbacher KJ, Maheswaran S, Haber DA, Toner M. Proc Natl Acad Sci U S A. 2010; 107(43):18392–7. [PubMed: 20930119]
27. Hsu CH, Di Carlo D, Chen C, Irimia D, Toner M. Lab Chip. 2008; 8(12):2128–34. [PubMed: 19023476]
28. Shelby JP, Lim DSW, Kuo JS, Chiu DT. Nature. 2003; 425(6953):38–38. [PubMed: 12955132]
29. Kim Y, Pekkan K, Messner WC, Leduc PR. J Am Chem Soc. 2010; 132(4):1339–47. [PubMed: 20063880]
30. Kim Y, Joshi SD, Davidson LA, LeDuc PR, Messner WC. Lab Chip. 2011; 11(13):2182–8. [PubMed: 21528131]

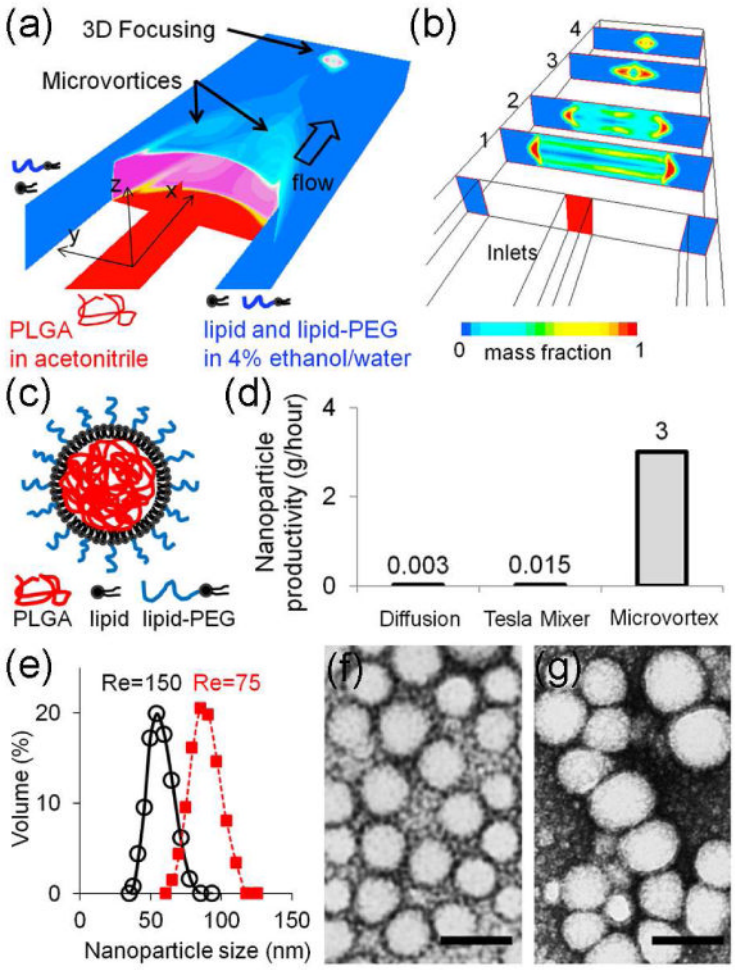

Figure 1. Mass production and size control of lipid-polymer hybrid (LPH) nanoparticles through controlled microvortices

(a, b) Schematic (a) and cross section views (b) of a simple, single-layer, and three-inlet microfluidic platform generating two symmetric microvortices and a 3D focusing pattern. **(c)** Illustrative structure of LPH nanoparticles synthesized in the microfluidic platform. **(d)** Microvortex nanoparticle synthesis shows 1000 times higher productivity than PLGA-PEG synthesis using diffusive mixing in a microfluidic flow-focusing pattern at a flow rate of 10 μL/min. Our microvortex approach enables 200 times faster production than previous lipid-polymeric nanoparticle synthesis using convective mixing in a Tesla Mixer. For comparison, the productivity (g/hour) represents the amount of PLGA (5 mg/mL) included in the produced nanoparticles, which was varied by altering the Reynolds number (Figure S3). After removing the free lipids by the purification process, the PLGA is assumed to be essentially 100% effective as previously reported.[4, 5] **(e)** Average distribution of the nanoparticles produced through the controlled microvortices. The average sizes are 55 nm (Re=150) and 81 nm (Re=75). The Reynolds number was computed by the microfluidic dimensions and flow rate used in the experiment (Figure S1). **(f, g)** Transmission electron microscopy (TEM) images that demonstrate the synthesized nanoparticles with two distinct sizes for Re=150 (f) and Re=75 (g) with only changes of flow rates (i.e. Reynolds number (Re)). The scale bars are both 100 nm.

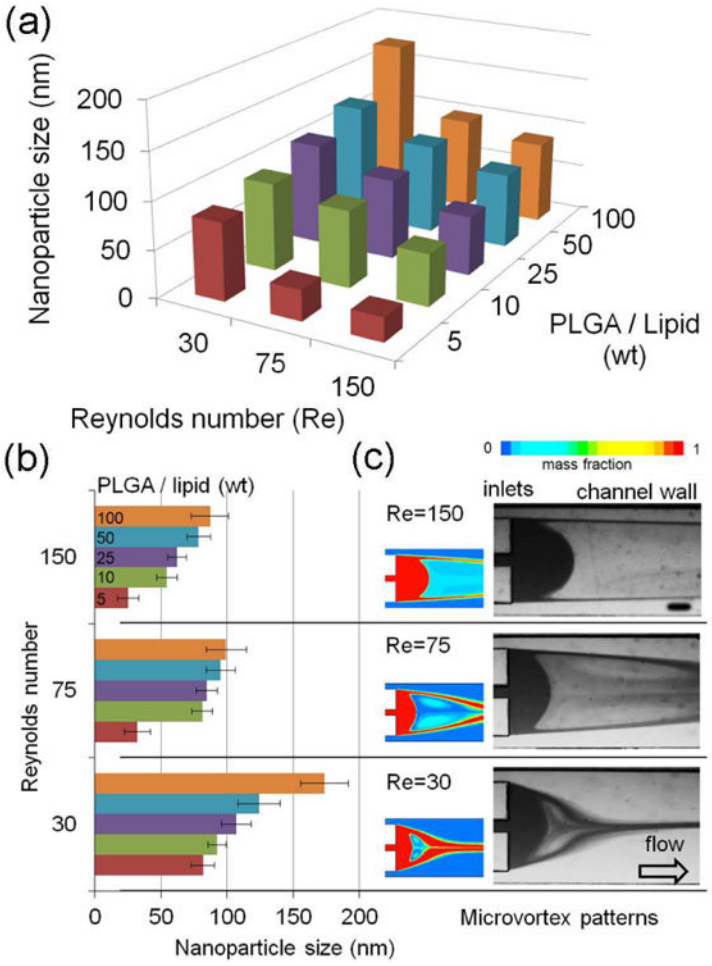

Figure 2. Size-controllable nanoparticle syntheses with variation of the Reynolds number in controlled microvortex patterns

(a) Nanoparticle size map controlled by varying Reynolds number with given PLGA-to-lipid weight ratios. The size represents the average value in the monodisperse distribution that occupies more than 85% of the overall volume of the produced nanoparticles (Figure S4). **(b)** Nanoparticle size manipulated by controlled microvortex patterns that vary the polymer-lipid mixing times. Error bars are standard deviations of different nanoparticle batches (n=5). **(c)** Microvortex patterns predicted by the computational fluid dynamics simulations and visualized by microscopic images (Figure S5; for methods see Supporting Information). The patterns exhibited very good agreement between simulations and images. In simulation, the color map represents mass fraction of the polymer and lipid streams. In visualization, the central stream has a 10% black ink diluted with deionized water. The scale bar is 200 μm.

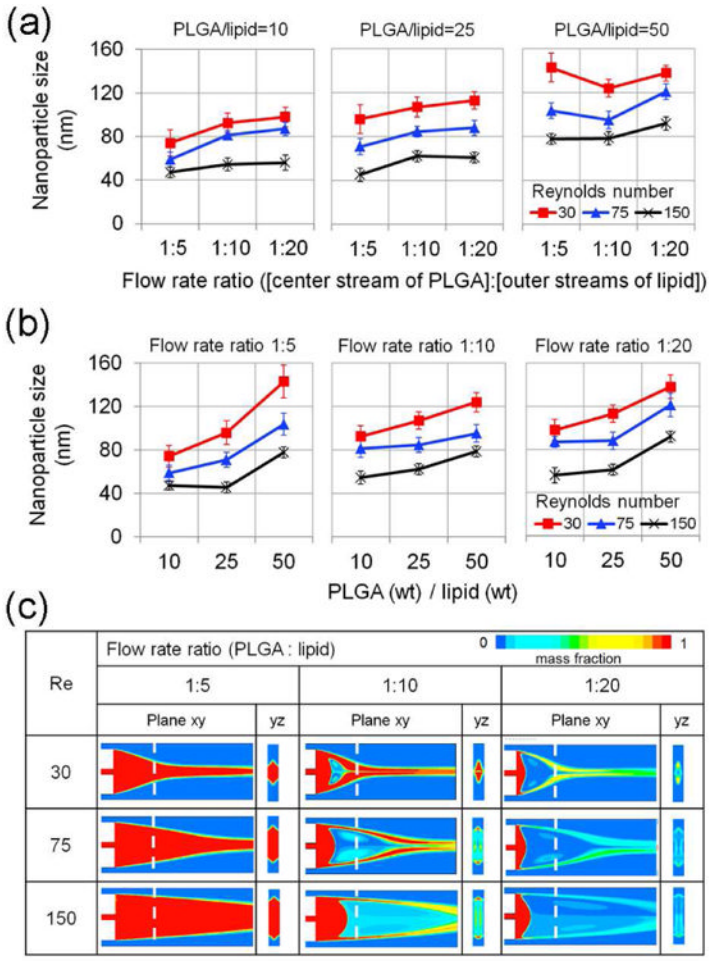

Figure 3. Nanoparticle size variations to controlled microvortex patterns

(a) Effect of flow rate ratios (1:5, 1:10, and 1:20) of [PLGA stream] to [outer lipid streams] on nanoparticle size with respect to Reynolds number (30, 75, and 150) and PLGA-to-lipid ratios (10, 25, and 50). **(b)** Effect of PLGA-to-lipid ratios (10, 25, and 50) on nanoparticle size with respect to Reynolds number (30, 75, and 150) and flow rate ratios (1:5, 1:10, and 1:20). Error bars are standard deviations of different nanoparticle batches (n=5). **(c)** Controllable microvortices in the xy and yz planes. In a flow rate ratio of 1:5, microvortex patterns were not well developed due to relatively higher portion of the central stream in the channel while the vortices were well developed in flow rate ratios of 1:10 and 1:20. Increasing the Reynolds number resulted in clearer microvortex formation while vortex patterns were undeveloped at Re=3 (Figure S5).

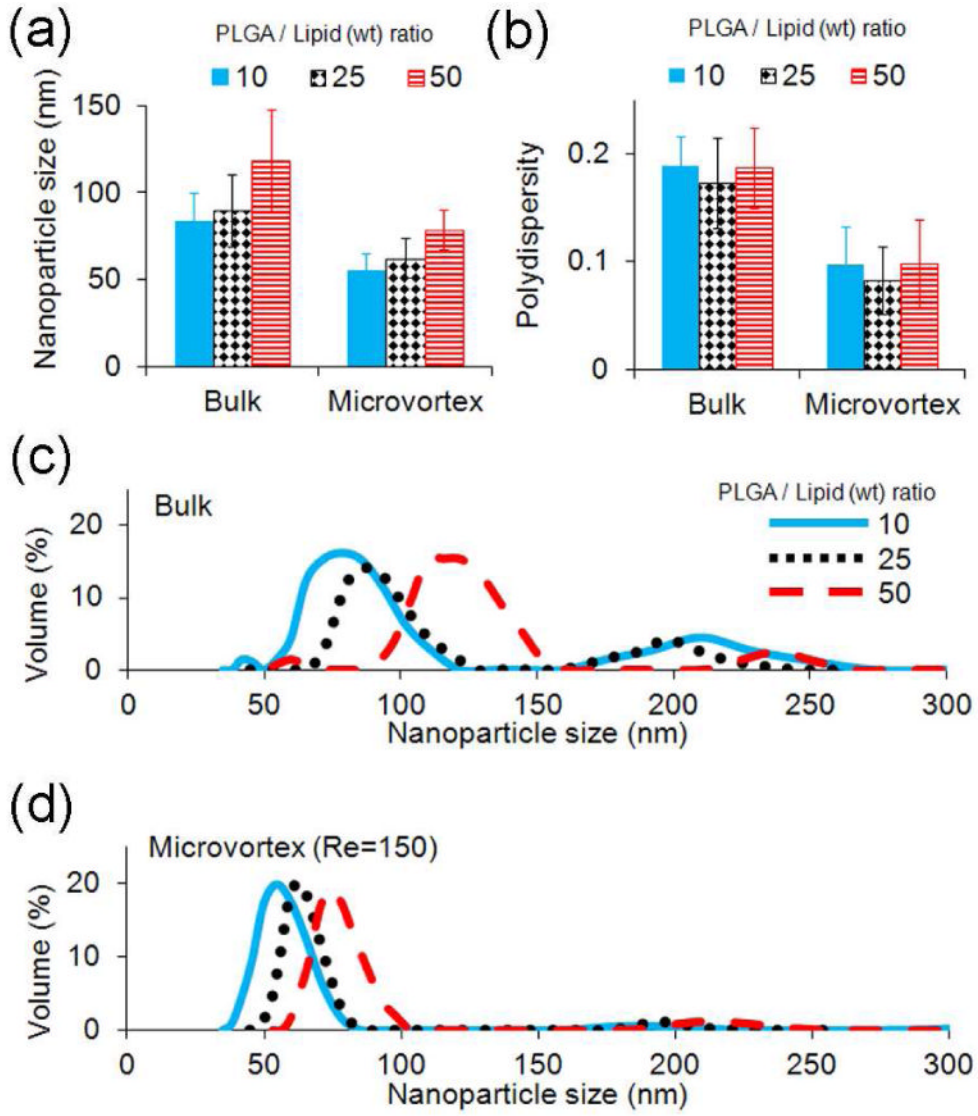

Figure 4. Comparison of nanoparticle size and distribution using two different approaches: bulk synthesis using conventional nanoprecipitation and microvortex mass production (Re=150)) with given PLGA-to-lipid weight rations of 10, 25, and 50

(a) Nanoparticle size. **(b)** Polydispersity of the average distribution. Error bars are both standard deviations of different batches (n=5). **(c, d)** Nanoparticle size distributions: (c) bulk and (d) microvortex. The solid, dotted, and dashed lines represent the PLGA-to-lipid weight ratios of 10, 25, and 50, respectively.

Table 1

Nanoparticle productivity as a function of the parameters: the flow rate, the Reynolds number, and the PLGA concentration. After removing the free lipids by the purification process, the PLGA is assumed to be essentially 100% effective as previously reported.[4, 5]

Total flow rates (mL/min)	Reynolds number (Re)	Nanoparticle productivity (g/hr)	
		PLGA = 1 mg/mL	PLGA = 5 mg/mL
2.2	30.6	0.13	0.65
5.5	76.4	0.33	1.65
11.0	152.8	0.66	3.30